A NONLINEAR CLUTCH SERVOMECHANISM FOR UNDERWATER CONTROL SURFACE ACTUATION

by

ROBERT J. CHENEY, JR.

A NONLINEAR CLUTCH SERVOMECHANISM FOR UNDERWATER CONTROL SURFACE ACTUATION

by

ROBERT J. CHENEY JR.

B.S. U.S. Coast Guard Academy
1960

SUBMITTED IN PARTIAL FULFILLMENT OF THE
REQUIREMENTS FOR THE
PROFESSIONAL DEGREE OF
NAVAL ENGINEER
AND THE DEGREE OF
MASTER OF SCIENCE IN ELECTRICAL ENGINEERING

at the

MASSACHUSETTS INSTITUTE OF TECHNOLOGY
August 1966

A NONLINEAR CLUTCH SERVOMECHANISM FOR UNDERWATER CONTROL SURFACE ACTUATION

by

ROBERT J. CHENEY, JR.

Submitted to the Department of Naval Architecture and Marine Engineering and the Department of Electrical Engineering on August 22, 1966 in partial fulfillment of the requirements for the professional degree of Naval Engineer and the degree of Master of Science in Electrical Engineering.

ABSTRACT

A nonlinear clutch type servomechanism is proposed to position the control surfaces of an underwater vehicle in accordance with specified performance criteria.

Two system configurations are discussed and compared:

(1) A two-state system employing pulse width angular velocity modulation on counter rotating clutches.

(2) A three-state system employing counter rotating clutches and a brake with error sampling.

Steady state load vibration will be present in each case. The degrading effects of these vibrations are developed and discussed.

Clutch power dissipation phenomena are discussed.

Actuator specifications are examined in light of overall system dynamics.

The present state of clutch technology is examined to fulfill system requirements.

Thesis Supervisor: George C. Newton, Jr.

Title: Professor of Electrical Engineering

TABLE OF CONTENTS

LIST OF FIGURES

CHAPTER I

INTRODUCTION AND SUMMARY

1.0 PROBLEM STATEMENT

Switching amplifiers, in general, offer higher efficiency and higher power per unit weight and volume than do continuous amplifiers. This research investigated the application of clutch type actuators operated in a switching mode to the feedback position control of the control surfaces of an underwater vehicle. The vehicle was assumed to be operating at maximum speed.

1.1 SYSTEM CONFIGURATION

A self-propelled underwater vehicle when properly designed with neutral stability in yaw-rate will exhibit fastest response in that mode of motion. A control surface position servo satisfying the requirements of yaw-rate tracking will be adequate for roll and depth control.

A linear small signal model for the yaw-rate loop is indicated in Fig. 1.1(a).

The individual transfer functions are

$$\frac{\dot{\psi}_o}{\delta_o} = \frac{A(s+a)}{s(s+b)(s+c)}$$

$$\frac{\delta_o}{\delta_i} = \frac{\omega_n^2}{s^2 + 2\zeta\omega_n s + \omega_n^2}$$

where K_1, K_2 are preassigned gain factors

A, a, b, c are speed dependent vehicle parameters

ω_n = natural frequency of servo actuator system

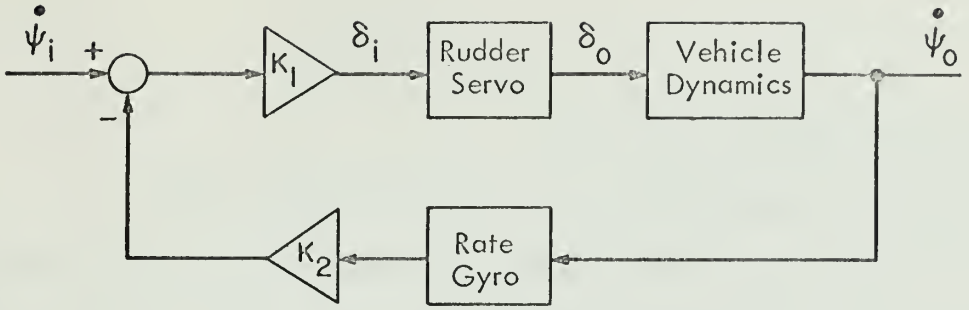

Fig. 1.1 (a) Yaw-Rate Loop

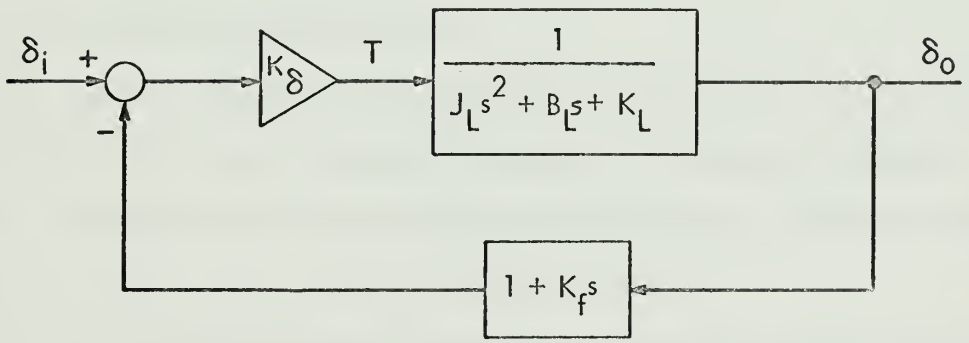

K_δ = TORQUE AMPLIFIER GAIN FACTOR

$J_L = 0.08 \frac{\text{in-\# sec}^2}{\text{radian}}$ LOAD INERTIA WITH ADDED HYDRODYNAMIC ENTRAINMENT

$B_L = 5 \frac{\text{in\# sec}}{\text{radian}}$ LOAD VISCOUS AND HYDRODYNAMIC FRICTION

$K_L = 1910 \frac{\text{in \#}}{\text{radian}}$ LOAD RESTORING TORQUE SINCE CONTROL SURFACE SUPPORT IS FORWARD OF QUARTER CHORD

K_f = RATE FEEDBACK GAIN FACTOR TO GIVE 0.5 DAMPING RATIO

Fig. 1.1 (b) Control Surface Actuator

ζ = damping ratio

$\dot{\psi}_i$ = command yaw rate

$\dot{\psi}_o$ = vehicle yaw rate

δ_i = command rudder deflection

δ_o = actual rudder deflection

A linear model for the control surface position control system is indicated in Fig. 1.1(b). The control surface system frequency response has been specified as flat to 7 cps with -3dB point at 27 cps.[2] The torque amplifier K_δ must deliver up to 1000 in -lb torque at a maximum speed of 100 RPM.

1.2 ACTUATOR CONFIGURATION

The design of a linear control system for control surface positioning is straightforward and can be realized with an electric or hydraulic actuator. These devices have inherent disadvantages, notably energy conversion in the former and shelf life in the latter.

Clutch type actuators offer superior performance in many respects although analysis is difficult due to nonlinear describing equations. Counter rotating clutch actuators can be operated in a push-pull fashion or in a switching mode. The former is undesirable from efficiency and heat sinking considerations. Switching operation is considered in this research.

Two basic configurations are considered: A two-state pulse width modulated counter-rotating clutch arrangement and a three-state system utilizing two counter-rotating clutches and a brake with state determined by sampled errors.

The two-state system is functionally diagrammed in Fig. 1.2(a).

The pulse width modulator output is designed to operate at a constant recurrence rate with fixed output magnitude positive or negative with half cycle duration determined by input level.[3] The pulse width modulator output drives the actuation mechanism of the clutch.

High inertia clutch input members are driven at constant speed from the vehicle prime mover. Assume that input and output members become instantly locked on signal from the pulse width modulator. The clutch output member velocity will be a square wave. The spring K_f transforms this velocity square wave into a triangular torque wave whose short-time mean level is transmitted to the load. The load and filter inertia attenuate torque components at switching frequency and higher harmonics.

Compensation and feedback networks insure reset action and stabilize the system. Reduction gearing is necessary to reduce clutch size.

In the steady state the clutch output velocity will be a symmetrical square wave. Some wobble will be inherent in the control surface load at switching frequency and its harmonics.

The three state system operation is self explanatory in Fig. 1.2(b). System operation is quite similar to that of the two-state configuration. The notable exceptions are the more complicated decision box and lack of steady state output oscillations at the expense of steady state errors, e. Limit cycle oscillations can occur at sampling frequency if the forward loop gain is high enough.

Detailed design of the clutch actuator system is the subject of a separate thesis and will not be dealt with here.

The advantages of clutch type actuators derive from the high torque squared-to-inertia ratios and low control power requirements. Shelf life is no problem with clutch servos.

The disadvantages of both configurations include heat dissipation at contact surfaces and output wobble with the possibility of exciting structural resonance.

Selection of the optimum switching of sampling frequency will involve tradeoffs between output wobble amplitude, which will decrease with switching frequency, and power dissipation in the clutches, which will increase with switching frequency. The fundamental switching frequency must lie above load resonance and away from structural resonances.

1.3 CONTROL SURFACE

The adverse effects of control surface wobble were investigated and acceptability criteria were assigned.

Control surface wobble manifests itself as a perturbation on the control surface angle of attack. The hydrodynamics of the situation were examined. Since mean incidence remains unchanged the dynamic lift of the control surface is not affected. Viscous drag effects were second order in magnitude, in fact, with the proper phasing and correct relationship between frequency, vehicle velocity and control surface chord length, propulsion will result. Cavitation inception was considered unlikely since the disturbance velocities were insignificant compared with quasi-steady levels.

Sound generation by the oscillating control surface proved to be a significant result. The sonic intensity level can be determined from the equation

$$I(r) = \frac{\overline{(\frac{dL}{dt})^2}\cos^2\theta}{16\pi^2\rho_o c_o^3 r^2} \quad \text{watts/m}^2$$

where L = lift force exerted by hydrofoil

θ = angle between direction of observation and lift force

ρ_o = density of undisturbed fluid

c_o = speed of sound in undisturbed fluid

r = distance from source to observer

This relationship is developed in Chapter Two. Thus, knowing lift as a function of angle of attack and angle of attack as a function of time, the sonic intensity can be obtained. The sound pressure level (SPL) can be obtained from intensity. A convenient measure of sound is the source level (far field radiation extrapolated to $r = 1M$) expressed in decibel ratio to 0.002 microbar (2×10^{-5} Newton/Meter^2).

For a given maximum control surface rate specification (100 RPM in this case) the source SPL can be determined as a function of switching frequency in the two-state configuration. A limit cycle amplitude determination must be made for the three-state configuration.

The two-state source SPL was observed to decrease 20 dB per decade of switching frequency.

1.4 CLUTCH POWER DISSIPATION

Referring to Fig. 1.2(a) if K_f were zero, the amount of energy necessary to accelerate the clutch output member from full clockwise angular velocity is

$$E_d = J_c \Omega^2 \text{ joules}$$

J_c = clutch output inertia

Ω = angular velocity of input members

Since this operation is performed twice in a switching period,

$$P_d = 2 J_c \Omega^2 f_{sw} \text{ watts}$$

f_{sw} = switching freq (cps)

The dissipation rating of the clutch must lie above this level. The situation can be alleviated somewhat by making K_f as stiff as possible without exceeding clutch pullout torque in spring windup. An analog simulation bears this out (see Fig. 4.1(b)). This result is consistent with two-state system design objectives in that clutch pullout torque must be higher than the greatest demanded.

In the analog simulation the filter inertia J_f (Fig. 1.2(a)) was considered infinite. In the actual system $J_f > 5J_c$ for efficient filtering so this assumption was not a bad one. The simulation is detailed in Chapter Four.

Since power dissipation is a linear function of switching frequency and a quadratic function of input member speed the gear ratio should be selected to minimize input member speed. Unfortunately load torque requirements determine the gear ratio since the clutch dimensions must be kept small. Pullout torque is determined by clutch size.

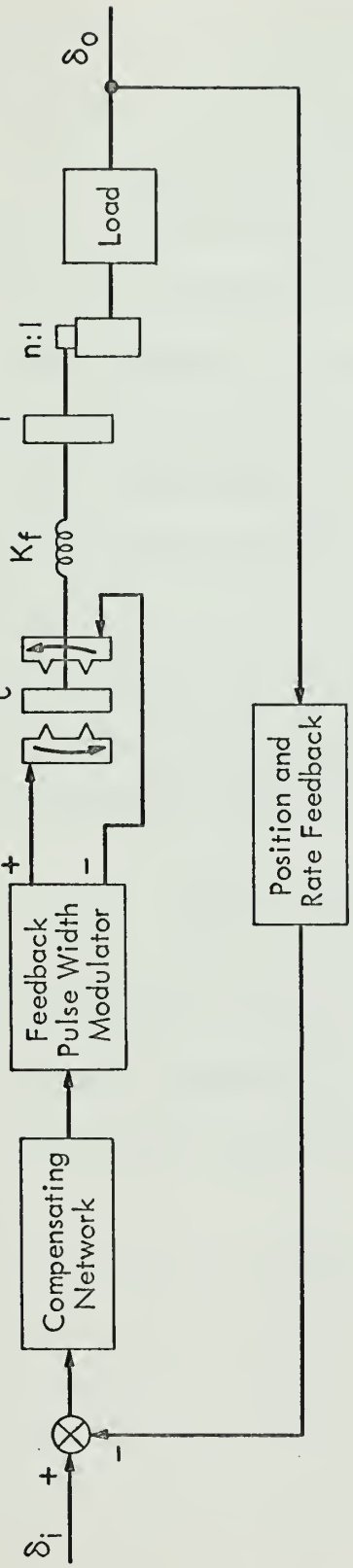

Fig. 1.2 (a) Two State Clutch Servo with Pulse Width Modulation

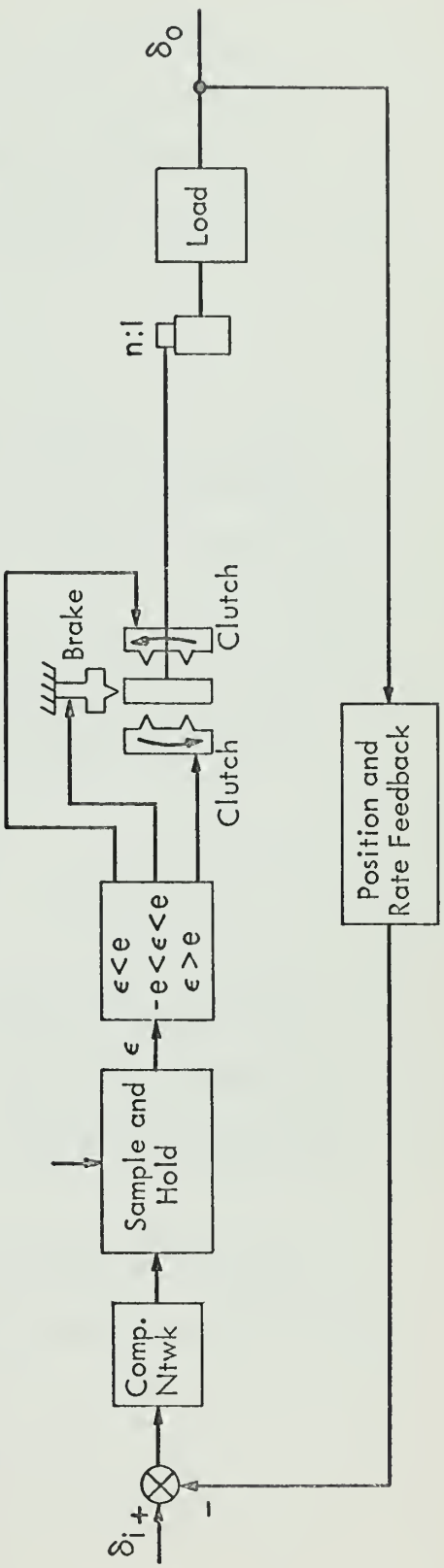

Fig. 1.2 (b) Three State Clutch Servo Configuration

If the control surface can be pivoted nearer to its center of pressure the output torque required (1000 in-lbs) will be reduced and the necessary reduction ratio can be reduced permitting lower clutch input member speed while maintaining maximum control surface position rate at the specified 100 RPM.

1.5 OVERALL SYSTEM DYNAMICS

Since the control surface servo is embedded within the overall vehicle dynamic control loop, a study was carried out to determine the effect of actuator bandwidth reduction on the dynamics of the total system.

The vehicle exhibits fastest behavior in the yaw rate loop (Fig. 1.1(a)). The control surface servo system was modelled as a second order system with damping ratio equal to $\frac{1}{2}$.

$$\frac{\delta_o}{\delta_i} = \frac{\omega_n^2}{s^2 + \omega_n s + \omega_n^2}$$

It can be shown that damping ratio = 0.5 minimizes integral square error for a linear position servo for a step input. This behavior can be achieved by proper selection of forward loop gain and output rate feedback.

Bode plots of the open yaw-rate loop were constructed for the specified servo and three slower servos. These data were transferred to a Nichols chart for comparison (Fig. 1.5).

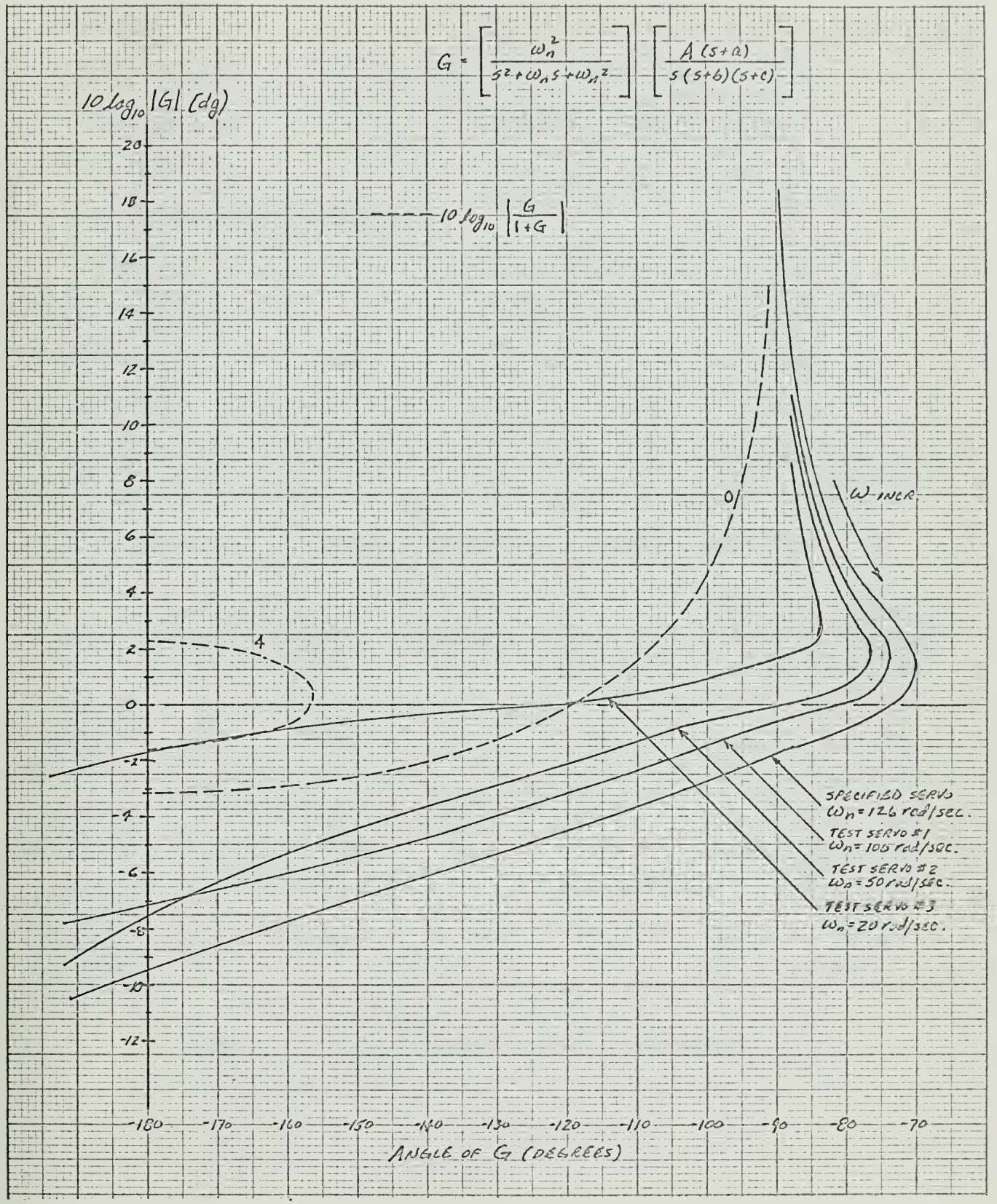

Fig. 1.5 Nichols Chart of Yaw-Rate Loop Frequency Response

It was concluded that the response speed of the control surface actuator could be halved without degrading the closed yaw-rate loop performance.

1.6 CLUTCH SPECIFICATIONS

The state of clutch technology was scanned and unfortunately present production line clutches do not fulfill system requirements. Switching rates in the range 75 to 150 cps are necessary for the two state system. This gives rise to an input-output rise time of one or two milliseconds. This demand has been met by very small instrument magnetic particle clutches. Figure 1.6 compares characteristics of three production devices with proper torque and speed characteristics.

Clutch Type	Maximum Torque (in-lb)	Maximum Speed (RPM)	Maximum Dimension (in)	Rise Time (m sec)	Output Inertia (in-lb sec^{2}x10^4)	Dissipation Rating (watts)
Solenoid-Operated Mech. Friction	60	7500	3.7	30	6.93	136
Magnetic Particle	35	3400	3.1	30	2.37	75
Solenoid-Actuated Vacuum-Operated Mechanical	60	1800	5	8	9.3	127

Fig. 1.6 Comparative Clutch Characteristics

In addition, the magnetic particle clutch exhibits 0.6 in-lb drag torque at zero excitation and the vacuum-operated clutch requires a small vacuum pump.

It may be concluded that the two-state actuator configuration is not technically feasible at present. Since the three-state system has not been fully investigated, a working model may be constructed using the present clutch technology. High speed magnetic tape drives have indicated a need for fast mechanical clutches and current research may evolve a device capable of meeting the requirements of the two-state actuator system.

CHAPTER II

SOUND GENERATION

The intensity of sound resulting from a lifting body in fluid flow has been investigated.[4] Rayleigh has shown that any frequencies in a fluid flow are equal to those of the sound generated.

Lighthill has considered the equations of motion of fluids and compared them with the equations of sound propagation in a medium at rest. The exact equations for the former may be written in the form

$$\frac{\partial^2 \rho}{\partial t^2} - C_o^2 \nabla^2 \rho = \frac{\partial^2}{\partial x_i \partial x_j} T_{ij} \qquad (2.1)$$

where $T_{ij} = \rho v_i v_j + p_{ij} - C_o^2 \delta_{ij}$

ρ = density

p_{ij} = compressive stress tensor

C_o = sonic velocity in fluid at rest

v_i = velocity component in direction x_i $(i = 1, 2, 3)$

Physically, this means that sound is generated by a fluid flow exactly as in a uniform medium at rest which is acted upon by externally applied fluctuating stresses. If we regard the flow as known it is possible to evaluate the sound generated.

Equation (2.1) is the non-homogeneous wave equation. The most general solution (Stratton 1941) is

$$\rho(\vec{x}) - \rho_o = \frac{1}{4\pi C_o^2} \int_v \frac{\partial^2 T_{ij}}{\partial y_i \partial y_j} \frac{d\vec{y}}{|\vec{x} - \vec{y}|} + \frac{1}{4\pi} \int_s \frac{1}{r} \frac{\partial \rho}{\partial n} + \frac{1}{r^2} \frac{\partial r}{\partial n} \rho + \frac{1}{c_o r} \frac{\partial r}{\partial n} \frac{\partial p}{\partial t} \, dS(\vec{y})$$

In this equation $\frac{\partial^2 T_{ij}}{\partial y_i \partial y_j}$, $\frac{\partial \rho}{\partial n}$, ρ, $\frac{\partial \rho}{\partial t}$ are taken at retarded times $t - \frac{r}{c_o}$, where $r = |\vec{x} - \vec{y}|$ and $\vec{n}$ is the outward normal from the fluid. The first integral is taken over the total volume V external to the solid boundaries and the second integral is taken over the surface S of the solid boundaries.

Curle has shown that the solution may be simplified under the assumption that:

(1) $|\vec{x}| >> \lambda$ ("far field" approximation)

(2) the solid boundaries are rigid, i.e., non-dilatational

(3) the flow is incompressible (Mach No. << 1)

Under these assumptions the solution reduces to

$$\rho - \rho_o = \hat{\rho} = \frac{1}{4\pi c_o^3} \frac{x_i}{x^2} \frac{\partial}{\partial t} F_i(t)$$

where $F_i(t) = \int_S P_i(\vec{y}, t)\, dS(\vec{y})$, the total resultant force exerted on the fluid by the solid boundaries.

In acoustic media, the sound pressure field is proportional to the density fluctuation field by the constant c_o^2 thus

$$\hat{p} = \frac{1}{4\pi c_o} \frac{x_i}{x^2} \frac{\partial}{\partial t} F_i(t)$$

This is the radiation field of a dipole source with axis parallel to F(t) the net resultant force exerted on the fluid by the boundaries. Rewriting in more convenient variables:

$$\hat{p} = \frac{1}{4\pi c_o} \frac{\cos\theta}{r} \frac{\partial}{\partial t} F_i(t) \qquad (2.2)$$

where θ is the angular distance between the radius vector r and the axis of $F_i(t)$.

Since intensity is defined as the acoustic power transmitted through a unit area

$$I = \frac{\overline{p^2}}{\rho_o c_o}$$

$\overline{p^2}$ = mean square acoustic pressure (Newtons/M^2)

$\rho_o c_o$ = characteristic impedance of acoustic medium (MKS RAYLS)

Generally it is more physically meaningful to consider a decibel ratio referred to a datum level for intensity and pressure measurements. A customary quantitative measurement in underwater acoustics is the source level sound pressure level. This is defined as

$$SPL = 10 \log_{10} \frac{\overline{p^2}}{p_o^2} \text{ dB}$$

where $\overline{p^2}$ is far-field acoustic mean square pressure extrapolated to a radial distance of one meter from the source, the reference pressure being 0.0002 microbar ($2 \times 10^{-5} N/M^2$) for underwater noise measurements.

If the force exerted by the body on the fluid can be determined then the SPL can be calculated.

CHAPTER III

HYDRODYNAMICS AND CONTROL SURFACE OSCILLATION

Principles of incompressible, non-cavitating hydrodynamics can be utilized to determine the external forces acting upon the fluid which will yield the sound pressure field. Sound generated by the oscillating control surface only is considered. This sound pressure will be additive to any presently inherent in vehicle operation exclusive of the control surface system.

In Equation (2.2), $F_i(t)$ must be determined to find the SPL. This total force exerted by the body on the fluid is due primarily to dynamic lift directed normal to the approach flow. A secondary force is due to viscous drag which is oriented parallel to the approach flow and generally equal to about one twentieth of the lift in magnitude.

For an oscillating hydrofoil the oscillating component of lift is a function of approach velocity, hydrofoil geometry, fluid density, and the magnitude and frequency of the oscillation. For a steady hydrofoil the dynamic lift is a function only of approach velocity, foil geometry, fluid density and angle of incidence with approach flow. A frequently used dimensionless parameter is the lift coefficient C_L.[5]

$$C_L = \frac{L}{\frac{\rho}{2} S U^2} = K\alpha \quad (-17^\circ < \alpha < 17^\circ)$$

for a symmetrical thickness form.

where L = dynamic lift

ρ = fluid density

S = area of foil in the span-chord plane

U = approach flow velocity

α = radian angle of attack

K = proportionality constant dependent on aspect ratio

The aspect ratio is the ratio of span squared to foil area S. For two dimensional flow (infinite aspect ratio), $K = 2\pi$. For zero aspect ratio (chord length much greater than span), $K = \pi/2$. It is known that at reduced frequencies greater than 0.5 the oscillating component of the flow becomes two-dimensional.

$K = \frac{\omega c}{2U}$ = reduced frequency

ω = radian frequency of oscillation

$\frac{c}{2}$ = semi-chord length

U = approach flow velocity

In the course of a mathematical investigation of wing flutter phenomena, Theodorsen[6] has shown that

$$\frac{L_{osc}}{L_{stdy}} = C(k) = \frac{H_1^{(2)}(k)}{H_1^{(2)}(k) + jH_o^{(2)}(k)}$$

for a lifting surface in rotary oscillation.

where L_{osc} = complex value of oscillatory lift component

L_{stdy} = quasi-steady lift corresponding to maximum inclination

$H_n^{(2)}$ = Hankel function of second kind of order n

The function C(k) is plotted in Fig. 3.1. Its behavior is quite similar to that of a lag network. The reduced frequencies of the vehicle control surface in the range of interest were found to be greater than 1.0 so that C(k) was assumed equal to $[0.5 + j0.0]$ throughout the analysis.

The foregoing conclusions have been predicated on the assumption that the foil is oscillating in a sinusoidal fashion with time.

Referring to Fig. 1.2(a), assume that the clutch is perfect in that the output member locks on with the appropriate input member at the switching instant. The angular velocity of the clutch output member will be a square wave with half-cycle duration determined by the pulse width modulator input. A Fourier decomposition of this signal yields:

$$\Omega_C(t) = \sum_{m=-\infty}^{\infty} F(m)\, e^{jm\omega_1 t}$$

$$F(m) = \begin{cases} \dfrac{2A(1-e^{-jm\omega_1\tau})}{jm\omega_1} & ;\ m \neq 0 \\ (2\,\frac{\tau}{T} - 1)A & ;\ m = 0 \end{cases}$$

where Ω_c = clutch output member angular velocity

ω_1 = switching rate (rad/sec)

A = magnitude of input member speed

τ = duration of positive half-cycle of PWM output

m = harmonic index

T = period of PWM output

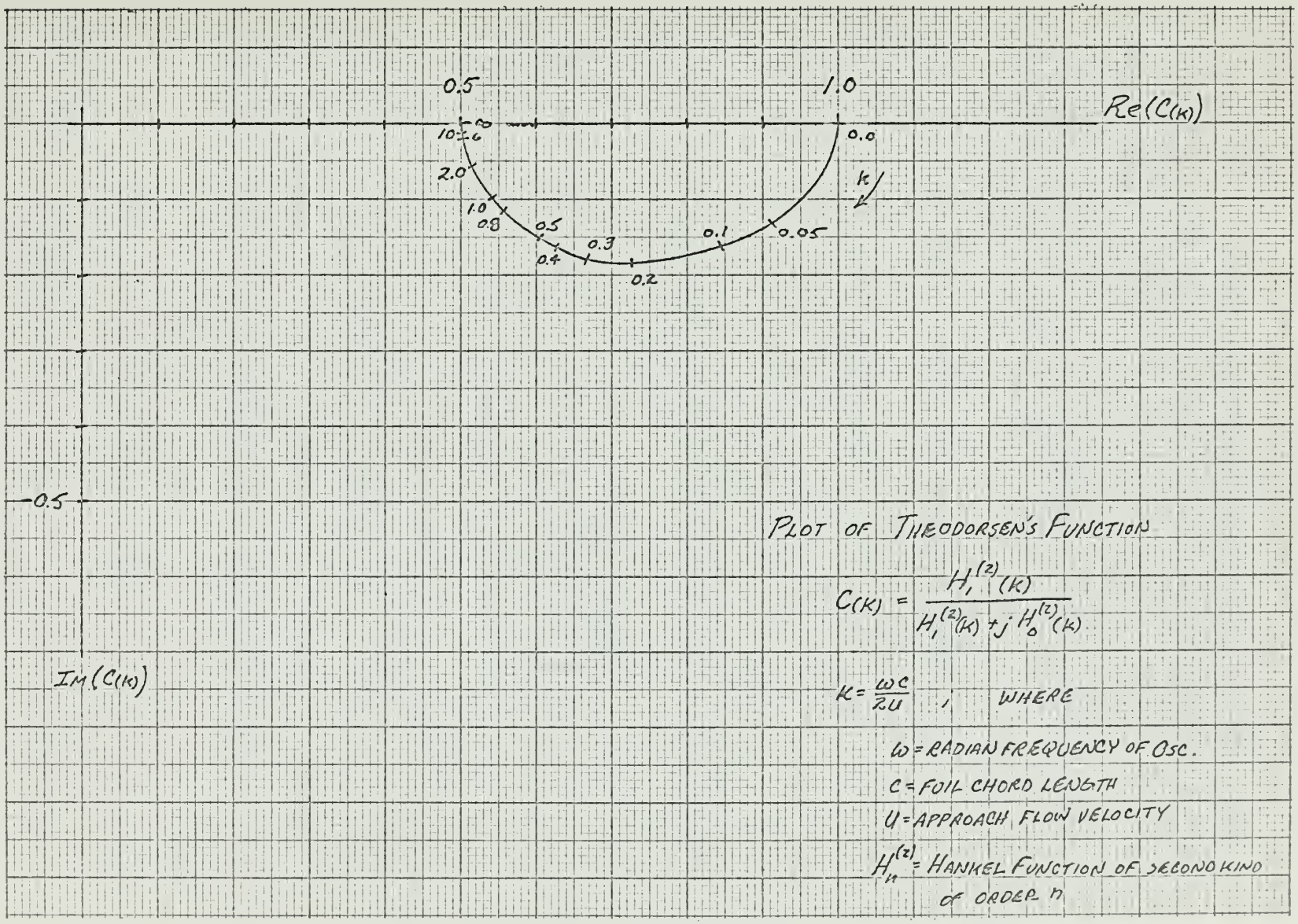

Fig. 3-1 Theodorsen's Function

In the case of steady state zero position error, $\tau = \frac{T}{2}$. The magnitude of the fundamental component of clutch output velocity will be a maximum of $\frac{4A}{\omega_1}$.

Referring again to Fig. 1.2(a) relations between control surface output velocity and clutch velocity can be written:

$$\frac{\Omega_C}{\Omega_L} = \frac{sZ_L}{n}\left(\frac{1}{K_f}\right) + n\left[1 + \frac{s^2 J_f}{K_f}\right]$$

where Z_L = load impedance

n = reduction ratio

s = complex frequency

For switching frequencies above load resonance (25 cps), inertia terms dominate and $Z_L \rightarrow sJ_L$.

Recombining: $$\frac{\Omega_c}{\Omega_L} = n\left[1 + \frac{s^2\left(J_f + \frac{J_L}{n^2}\right)}{K_f}\right]$$

Examining the relative magnitudes of inertias:

$$J_f \approx 3 \times 10^{-3} \text{ in lb sec}^2 \quad (3\text{-}5\ J_C \text{, see Fig. 1.6})$$

$$J_L = 8 \times 10^{-2} \text{ in lb sec}^2$$

since a reduction ratio of at least 15:1 will be required, the effects of reflected load inertia can be ignored with the result that

$$\frac{\Omega_L}{\Omega_C} = \frac{1}{n\left[1 + s^2 \frac{J_f}{K_f}\right]}$$

indicating that switching frequency harmonics will be attenuated inversely as the square of the order. Coupling this result with the $\frac{1}{m}$

character of the clutch output spectrum, the foil motion can be considered a pure sinusoid at fundamental switching frequency.

The source SPL can now be calculated

$$\overline{p^2}_{source} = \frac{\overline{(\frac{dL}{dt})^2}}{16\,\pi^2\,c_o^2}$$

where $L = L_{osc} \sin \omega_1 t = C(k)\ K_L [\theta_L \sin \omega_1 t]$

K_L = constant of lift-incidence proportionality

$K_L = \pi \rho S\ U^2$ (MKS units)

$C(k)$ = Theodorsen's function

Since the sound pressure is a result of vortex shedding, a measure of spanwise phase correlation is necessary. A good measure of phase correlation is obtained by a strip theory approach. The foil was arbitrarily subdivided into four spanwise sections. The Theodorsen function was found to be nearly invariant across the span so that the sound field was assumed 100 percent phase correlated. The tip vortex baffle increases the reliability of this assumption.

Converting the mean square pressure to decibel ratio

$$SPL_{source} = 20 \log_{10} (\Omega_L) + P_1 \quad dB$$

$$= 20 \log_{10} \left[\frac{\Omega_c}{n(1-\omega_1^2 \frac{J_f}{K_f})} \right] + P_1 \quad dB$$

P_1 contains K_L; $C(k)$, reference pressure (0.002 μb), $(0.707)^2$, $16\,\pi^2$ and C_o^2.

If we further assume that $\frac{\Omega_c}{n} = 100$ RPM (specified maximum control surface speed), then

$$SPL_{source} = P_2 - 20 \log_{10} \omega_1 (1-\omega_1^2 \frac{J_f}{K_f})$$

This relationship is plotted in Fig. 3.2 for various ratios of switching frequency to $\sqrt{\frac{K_f}{J_f}}$.

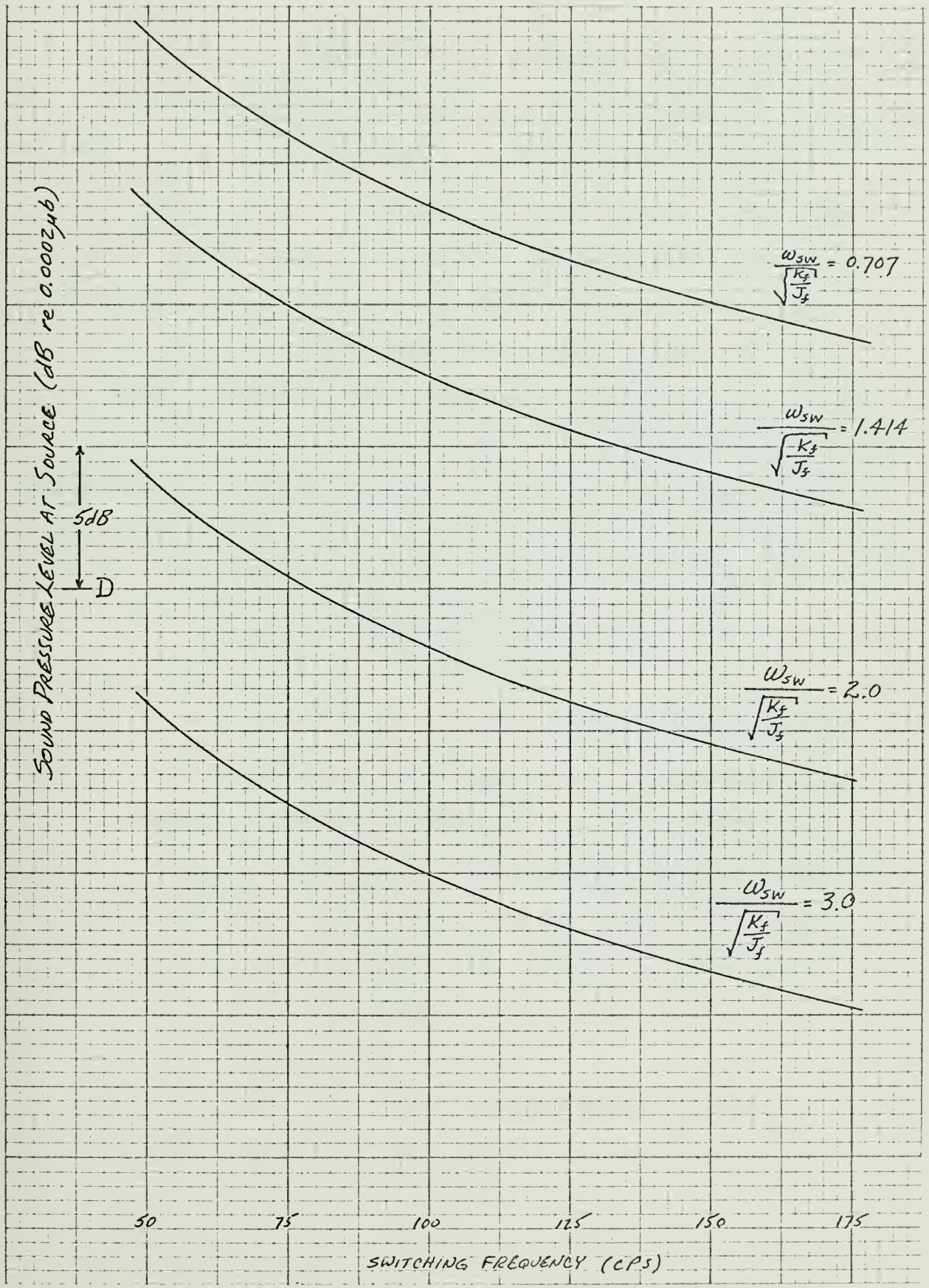

Fig. 3.2 Source SPL vs Switching Frequency

CHAPTER IV

CLUTCH POWER DISSIPATION

As mentioned in Section 1.4 power is dissipated in the interval between the switching instant and the point at which clutch input and output members become locked. The instantaneous dissipation is the product of pullout torque and slip speed. The time average power dissipated will be approximately twice the product of clutch output inertia, input member speed squared and switching rate.

In order to minimize power dissipation, the absolute value of slip velocity must be minimized. Assuming J_c , J_f and switching frequency fixed (see Fig. 1.2(s)), the effect on slip velocity of varying K_f was observed on an analog simulation. Since J_f will be three to five times greater than J_c , J_f was assumed infinite for purposes of simulation. The system simulated and computing diagram are indicated in Figure 4.1(a).

The simulation was carried out on the Philbrick Analog Computer at the M.I.T. Engineering Projects Laboratory. Results are indicated in Figure 4.1(b). The input member velocity is the square wave. The output member velocity is the initially ramp-like square wave which tracks the input. The third trace is the amplified difference between the two. A small biasing error is evident in some of the computations. This is attributed to amplifier drift since it was necessary to saturate one amplifier in the loop.

From the simulation, it may be concluded that the spring K_f should be made as stiff as possible without exceeding clutch pullout

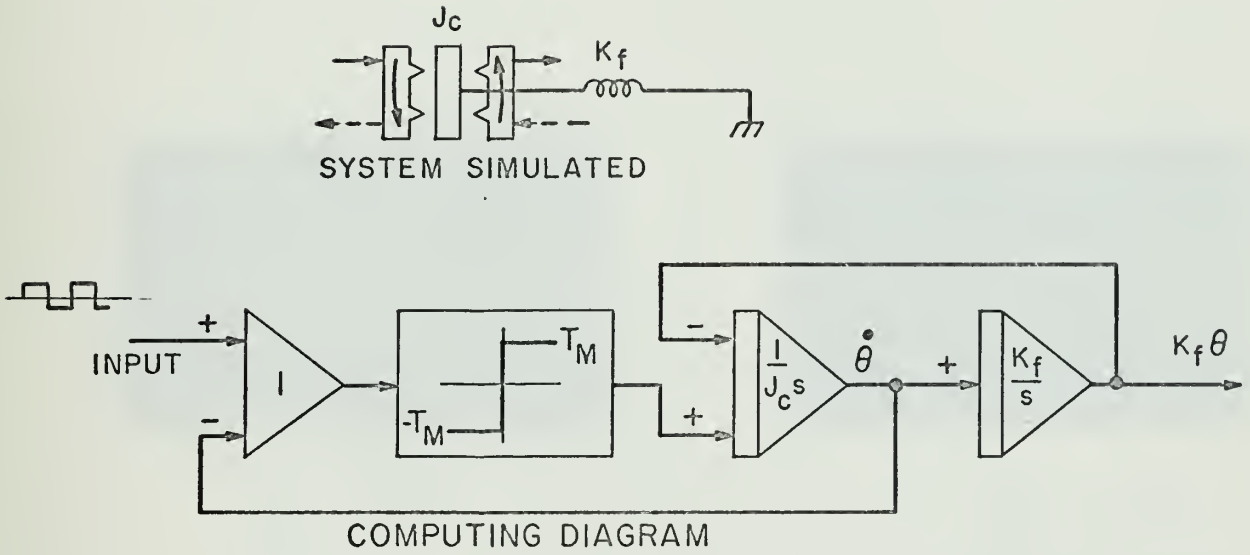

Fig. 4.1 (a) Analog Simulation of Clutch Dissipation Phenomena

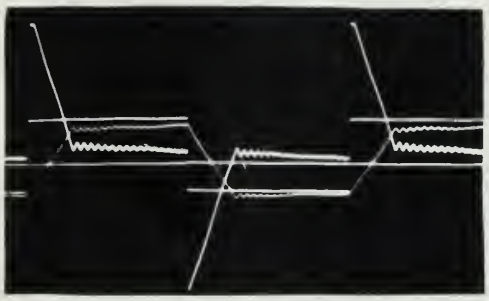

$\frac{\omega_n}{\omega_{sw}} = 0.478$

$\frac{\omega_n}{\omega_{sw}} = 1.21$

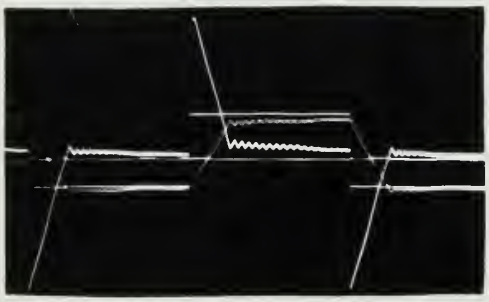

$\frac{\omega_n}{\omega_{sw}} = 0.735$

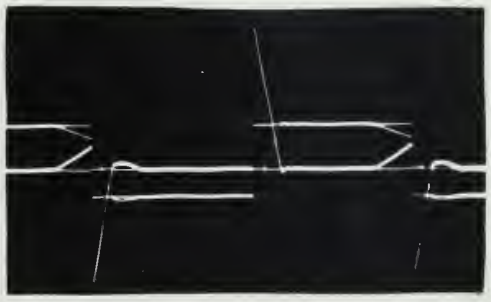

$\frac{\omega_n}{\omega_{sw}} = 1.385$

Note slip as spring is wound up to pullout torque

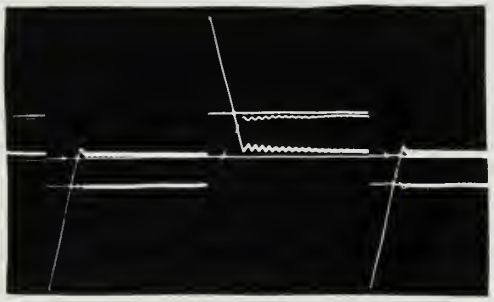

$\frac{\omega_n}{\omega_{sw}} = 1.0$

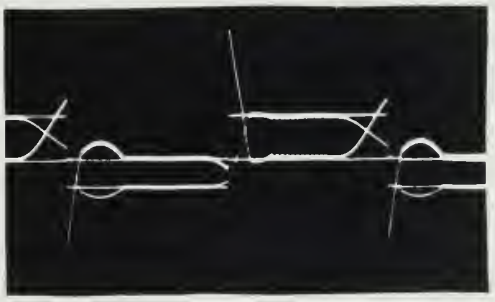

$\frac{\omega_n}{\omega_{sw}} = 1.54$

$\omega_n = \sqrt{\frac{k_f}{J_c}}$ ω_{sw} = switching freq.

Note slip as spring is wound up to pullout torque

Fig. 4.1(b) Response of Second Order Clutch Output System

torque in spring windup. At first glance, no differences may be apparent in Fig. 4.1(b). A closer examination reveals that response time for $\frac{\omega_n}{\omega_{sw}} = 1.21$ is about half that for $\frac{\omega_n}{\omega_{sw}} = 0.478$.

Input member speed and switching rate must be accounted for in the final selection of K_f.

BIBLIOGRAPHY

1. "The Hydrodynamic Design and Dynamic Control of the RETORC II, System Alpha Vehicles (U)"; H.M. Jensen, Penn. State Univ. ORL, June 15, 1965 (CONFIDENTIAL)

2. Specification for Electromechanical Actuator System, NUOS, No. 3.27.65/ASP:

3. "A Two-State Modulation System"; A.G. Bose, a Paper presented before the Western Electronic Show and Convention, San Francisco, August, 1963.

4. Curle, J.N., 1955 Proc. Roy. Soc. A, 231, p. 505.
   Lighthill, M.J., 1952 Proc. Roy. Soc. A, 211, p. 564.

5. Theory of Wing Sections, Abbott and Von Doenhoff, Dover, 1959.

6. "General Theory of Aerodynamic Instability and the Mechanism of Flutter"; T. Theordorsen, NACA Report, 496, 1935.